Inorganic Chemistry

Synthesis, Spectral Characterization and Crystal Structures of Five Organic Ammonium Tetrasulfidomolybdates

Bikshandarkoil R. Srinivasan,*[a] Sunder N. Dhuri,[a] Ashish R. Naik,[a] Christian Näther,[b] and Wolfgang Bensch[b]

Dedicated to Professor Koyar S. Rane on the occasion of his 72nd birthday

The syntheses, spectral characterization and crystal structures of five organic ammonium tetrasulfidomolybdates namely $(C_4H_{12}N)_2[MoS_4]$ **1** ($C_4H_{12}N$ is 2-methyl-propan-2-aminium), $(C_5H_{16}N_2)[MoS_4]$ **2** ($C_5H_{16}N_2$ is N^1,N^1-dimethylpropane-1,3-diaminium) $(C_5H_{16}N_2)[MoS_4]$ **3** ($C_5H_{16}N_2$ is N^1,N^3-dimethylpropane-1,3-diaminium) $(C_6H_{20}N_4)[MoS_4]$ **4** ($C_6H_{20}N_4$ is 2-amino-*N*-{2-[(2-ammonioethyl)amino]ethyl}ethanaminium and $(C_5H_{14}N_2)[MoS_4]\cdot{}^1/_2H_2O$ **5** ($C_5H_{14}N_2$ is 1-methylpiperazine-1,4-diium) are reported. The charge balancing cations in **1**–**3** are protonated methyl substituted propanamines, while the dications of **4** and **5** are derived from a tetraamine and a cyclic diamine respectively. The crystal structures of **1** to **5** consist of an unique tetrahedral $[MoS_4]^{2-}$ dianion charge balanced by a crystallographically independent organic dication for all compounds excepting **1** which contains a pair of unique (2-methylpropan-2-aminium) monocations. Although all the compounds are crystallized from aqueous solutions, **1** to **4** are anhydrous while **5** is a hemihydrate. In the crystal structures, the organic cations and the tetrasulfidomolybdate dianions are interlinked with the aid of several N–H···S and C–H···S hydrogen bonding interactions. In addition to N–H···S and C–H···S hydrogen bonds, compound **5** exhibits N–H···O and O–H···O hydrogen bonding interactions involving the H_2O molecule, which interlinks pairs of anions with pairs of cations. Hirshfeld surface analyses were performed which reveal distortion of the $[MoS_4]^{2-}$ tetrahedra, extensive S···H interactions between the anions and cations and also H···H contacts between the cations. A comparative study of the structural chemistry of thirty-eight tetrasulfidomolybdates is described.

1. Introduction

In a paper titled, "Ueber die Schwefelverbindungen des Molybdäns" Krüss[1] reported on several sulfur compounds of Mo. Although this work was published in 1884, a systematic study of the chemistry of the soluble sulfides of Mo and other early transition metals started much later after the synthesis of ammonium tetrathiomolybdate (tetrasulfidomolybdate is the name as per current IUPAC nomenclature) was included in Brauer's handbook of preparative inorganic chemistry.[2] A review article on thio and seleno compounds of the early transition metals by Diemann and Müller was published in 1973.[3] The investigations performed in the last five decades by several research groups have revealed the importance of sulfidomolybdates in diverse areas of science like hydrodesulfurization catalysis, bioinorganic chemistry, medicine, organic synthesis, and solid state ^{33}S NMR spectroscopy.[3–19]

As part of a long-standing research activity we have been investigating the synthetic chemistry and structural aspects of the group(VI) metal chalcogenides. Our contributions in this area have resulted in the synthesis, spectral characterization, and structural identification of several tetrasulfidomolybdates[20,21] and the corresponding W analogues,[22–24] charge balanced by organic ammonium cations. We have demonstrated that the structurally flexible $[MS_4]^{2-}$ (M = Mo, W) tetrahedron can exist in different environments.[20–24] For the preparation of these compounds different procedures are used. The most often applied method is based on the classic work of Krüss,[1] which involves the dissolution of the trioxide MoO_3 or ammonium heptamolybdate $(NH_4)_6(Mo_7O_{24})\cdot 4H_2O$ in aqueous ammonia followed by exhaustive treatment with H_2S gas to obtain red crystals of the bis(ammonium) salt $(NH_4)_2[MoS_4]$. The use of an alkyl amine instead of ammonia in the Krüss method affords the synthesis of compounds with general composition $(RNH_3)_2[MoS_4]$ (R = alkyl group). In our research, we have developed a base promoted cation exchange reaction applying $(NH_4)_2[MS_4]$ (M = Mo, W) as precursor for reaction with organic amines to obtain organic ammonium tetrasulfidometalates.[20–24] The syntheses can also be performed under solvothermal conditions affording formation of crystalline tetrasulfidomolybdates charge balanced by metal-organic cations.[25,26] An important structural feature of metal-organic or organic tetrasulfidomolybdates is an extended S···H hydrogen bonding

[a] Prof. B. R. Srinivasan, Prof. S. N. Dhuri, Dr. A. R. Naik
School of Chemical Sciences, Goa University, Taleigao Plateau, Goa, 403 206 India
E-mail: srini@unigoa.ac.in
[b] Prof. Dr. C. Näther, Prof. Dr. W. Bensch
Institut für Anorganische Chemie, Christian-Albrechts-Universität Kiel, Max-Eyth Strasse 2, D-24118 Kiel, Germany

Supporting information for this article is available on the WWW under https://doi.org/10.1002/slct.202100930

network between the anion and the cation with S–H distances shorter than the sum of the van der Waals radii of S and H.[27] These interactions can be varied by altering the steric bulk as well as the number of potential donor hydrogen atoms on the amine N atom of the organic cation. In this context we have undertaken this study by choosing five organic amine molecules (Scheme 1) which differ in terms of the number of hydrogen donors, to investigate the hydrogen bonding patterns and the resulting S···H networks.

In this manuscript, we describe the synthesis, IR and Raman spectra and crystal structures of five new organic ammonium tetrasulfidomolybdates (**1** to **5**). The charge balancing cations in **1**–**3** are based on methyl substituted propanamines (Scheme S1). 2-Methylpropan-2-amine used for the synthesis of (**1**) is a monoamine, while the isomeric diamines N^1,N^1-dimethylpropane-1,3-diamine and N^1,N^3-dimethylpro-pane-1,3-diamine employed for the synthesis of compounds (**2**) and (**3**) respectively differ in terms of the substitution on the amine functionalities. For **4** the charge balancing dication is derived from the tetraamine *N*,*N*'-bis(2-aminoethyl)ethane-1,2-diamine (trien). With this amine we have also prepared the corresponding W-analogue (**4**-**W**). Depending upon the protonation of the *N* atoms (amine or imine) of the tetramine different dications can form. For the synthesis of **5** the cyclic diamine 1-methylpiperazine was used. Details of synthesis are given in Supporting Information.

2. Results and discussion

2.1. Syntheses and spectra

The compounds described in this study were synthesized either by passing H_2S gas through an aqueous organic amine solution of molybdic acid (for **1** and **5**)[2,28] or by the base promoted cation exchange reaction using $(NH_4)_2[MS_4]$ (M = Mo for **2**–**4** or W for **4**-**W**) salts and the corresponding organic amine. All compounds are stable in dry air and analysed satisfactorily. Unlike $(NH_4)_2[MoS_4]$, which undergoes slow surficial degradation, the organic tetrasulfidomolybdates are quite stable and retain their red colour. All compounds are slightly soluble in water but freely soluble in aqueous ammonia, DMSO, DMF and insoluble in CH_3CN, CH_2Cl_2, toluene, alcohol. The compounds were characterized by UV-Vis spectra which confirm the presence of the tetrahedral $[MoS_4]^{2-}$ anion while the IR and Raman spectra serve to identify the organic cation and the anion as shown below.

The electronic spectra of the red colored compounds **1**–**5** are nearly identical and exhibit bands which can be assigned to the charge transitions of the $[MoS_4]^{2-}$ chromophore.[3,4] The longest wavelength of absorption occurs at ~470 nm for all the Mo compounds (Figure S1), while this signal is blue shifted to 394 nm for the $[WS_4]^{2-}$ compound (**4**-**W**). Compounds **1**–**5** and **4**-**W** exhibit several signals in their mid-infrared spectra above 500 cm^{-1} all of which originate from the organic cation, while the M–S vibrations of the $[MS_4]^{2-}$ anion are observed at lower energies below 500 cm^{-1} (Figure S2). For the free tetrahedral $[MS_4]^{2-}$ anion four characteristic vibrations $\upsilon_1(A_1)$, $\upsilon_2(E)$, $\upsilon_3(F_2)$ and $\upsilon_4(F_2)$ are expected. All four bands are Raman active while only υ_3 and υ_4 are IR active. When the tetrahedron is distorted, the symmetry is reduced and as a result the symmetric vibration $\upsilon_1(A_1)$ appears in the infrared spectrum at 481 cm^{-1} as a signal of medium intensity and an intense signal for the triply degenerate $\upsilon_3(F_2)$ asymmetric stretching M–S vibration at around 465 cm^{-1}.[29] The observed Raman bands of the $[MS_4]^{2-}$ unit are in the expected range and add credence to the infrared data (Figure S2). The formula of the compounds could be readily derived from the elemental analytical data and the $[MoS_4]^{2-}$ content, which indicates that the Mo:amine ratio is 1:2 in **1** and 1:1 for **2** to **5** and **4**-**W** indicating that a dication is formed in all these compounds. The analytical and spectral results thus indicate that in **4** (or in **4**-**W**) only two of the four N atoms of trien are protonated. Depending upon the protonation of the amine or imine nitrogen, four different structures are possible (see I to IV in Scheme 2) for a diprotonated trien.

In earlier work we reported partial protonation of a tetraamine or a triamine for the $[MoS_4]^{2-}$ salts of tris(2-aminoethyl) amine (tren),[21] and the triamines bis(2-aminoethyl)amine (dipn) and 2-piperazin-1ylethanamine.[30] For all these amines which form a 1:1 salt with $[MoS_4]^{2-}$ there is more than one possibility for a diprotonated cation. The correct structure type

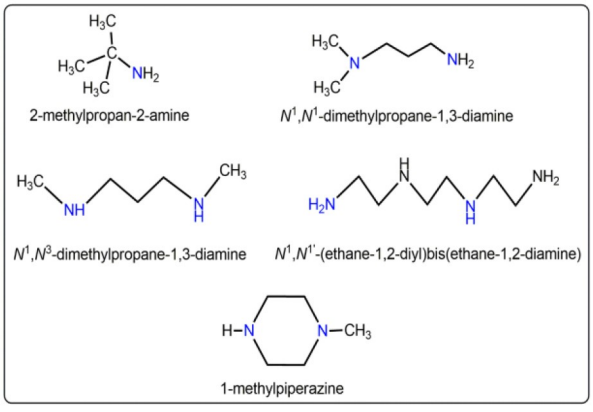

Scheme 1. The five different organic amines used in the present study.

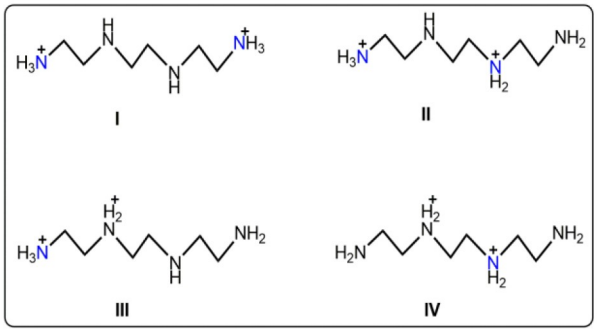

Scheme 2. Four different dications of *N*,*N*'-bis(2-aminoethyl)ethane-1,2-diamine (trien).

for the diprotonated cation was identified by the determination of the single crystal structure.

2.2. X-ray crystal structure determination

Intensity data were collected on a STOE-Imaging Plate diffraction System (IPDS 1) using graphite-monochromated Mo-Kα radiation. For compound **4** a numerical absorption correction was performed. The structures were solved with direct methods using SHELXS-97[31] and refinement was done against F^2 using SHELXL-2016.[31] All non-hydrogen atoms were refined anisotropically. The C–H and N–H hydrogen atoms were located in difference map but finally positioned with idealized geometry (methyl and ammonium H atoms allowed to rotate but not to tip) and refined isotropic with $U_{iso}(H) = 1.2\ U_{eq}(C,N)$ (1.5 for methyl and ammonium H atoms) using a riding model. In compound **4**, the positions of some of the N–H hydrogen atoms were taken from difference map. Their bond lengths were set to ideal values and finally they were refined isotropic with $U_{iso}(H) = 1.2/1.5\ U_{eq}(N)$ using a riding model. In compound **5** the O–H hydrogen atom was located in difference map, its bond lengths were set to ideal values and finally it was refined isotropic with $U_{iso}(H) = 1.5\ U_{eq}(O)$ using a riding model. In compound **3** two C atoms are disordered in two orientations and were refined using a split model and restraints. For compound **4** the absolute structure was determined and is in agreement with the selected setting (Flack X parameter: −0.039(43) by classical fit to all intensities and −0.031(24) from 1376 selected quotients (Parsons' method). The technical details of data acquisition and some selected refinement results are summarized in Table 1.

2.3. Description of crystal structures 1–5

The structure of **1** consists of two crystallographically independent 2-methylpropan-2-aminium cations and a tetrahedral $[MoS_4]^{2-}$ anion with all atoms located in general positions (Figure S3). In all other compounds (**2**–**5**), the structure consists of an unique $[MoS_4]^{2-}$ dianion and a crystallographically independent organic dication (Figures S4–S5). Compound **5** additionally contains a lattice water molecule located in a special position. In all compounds, the geometric parameters of the organic cations are in the normal range. For convenience the structures of **1**–**3** based on methyl substituted propanamines are discussed first followed by the structures of **4** and **5** which are based on dications of a tetraamine and a cyclic diamine respectively.

In **1** the $[MoS_4]^{2-}$ tetrahedron is slightly distorted with S–Mo-S angles ranging between 108.70(5) and 110.03 (5)°. The Mo–S bond lengths are from 2.1743(13) to 2.2038(11) Å (Table 2), with two bonds being shorter and two longer than the mean value of 2.1881 Å. The difference △ between the longest and the shortest Mo–S bond in **1** is 0.0295 Å. The analysis of the structure reveals that the $[MoS_4]^{2-}$ anion is linked to six different organic cations with the aid of several N–H···S and C–H···S interactions (Figure S3), while each crystallographically unique cation is hydrogen bonded to three different anions. A total of fourteen hydrogen bonds comprising of nine N–H···S bonds and five C–H···S interactions (Table 3)

Table 1. Selected crystal data and results of the structure refinements for compounds **1**–**5** and **4-W**.

Compound	**1**	**2**	**3**	**4**	**5**	**4-W**
Sum formula	$C_8H_{24}MoN_2S_4$	$C_5H_{16}MoN_2S_4$	$C_5H_{16}MoN_2S_4$	$C_6H_{20}MoN_4S_4$	$C_5H_{15}MoN_2O_{0.5}S_4$	$C_6H_{20}WN_4S_4$
MW/g mol^{-1}	372.47	328.38	328.38	372.44	335.37	460.35
Crystal system	Triclinic	Monoclinic	Monoclinic	orthorhombic	Monoclinic	orthorhombic
Space group	*P*	*C*2/*c*	$P2_1/n$	$Pca2_1$	*C*2/*c*	$Pca2_1$
a/Å	7.2228(11)	10.551(2)	7.2071(4)	16.7759(9)	14.4127(9)	16.848(3)
b/Å	11.050(2)	10.0746(19)	18.5371(13)	8.8850(7)	12.4254(10)	8.9475(18)
c/Å	11.527(2)	24.256(3)	9.6954(6)	9.5926(5)	13.8134(8)	9.6790(19)
α/°	110.919(12)	90	90	90	90	90
β/°	90.547(17)	93.533(15)	90.186(7)	90	102.257(7)	90
γ/°	91.159(17)	90	90	90	90	90
V/Å^3	859.1(3)	2573.5(8)	1295.29(14)	1429.81(16)	2417.4(3)	1459.1(5)
T/K	220(2)	293(2)	293(2)	170(2)	170(2)	170(2)
Z	2	8	4	4	8	4
D_{calc}/g cm^{-3}	1.440	1.695	1.684	1.730	1.843	2.096
μ/mm^{-1}	1.228	1.627	1.617	1.479	1.738	8.468
Crystalsize/mm	0.08×0.08×0.09	0.08×0.08×0.10	0.09×0.10×0.12	0.11×0.18×0.23	0.09×0.14×0.22	0.18×0.12×0.08
Tmin/max	–	–	–	0.7218/0.8454	0.7130/0.8222	–
θ_{max}	27.005	03.030	27.953	28.038	28.043	30.02
Refl. collected	8223	6244	12135	13329	13151	7374
Unique refl.	3710	3759	3065	3308	2873	3372
R_{int}	0.0865	0.0246	0.0272	0.0412	0.0315	0.0287
Refl. [$F_o > 4\sigma(F_o)$]	3040	3283	2636	3161	2565	3161
Parameters	145	113	119	138	116	138
$R_1[F_o > 4\sigma(F_o)]$	0.0477	0.0289	0.0276	0.0225	0.0270	0.0183
wR_2 (for all data)	0.1371	0.0756	0.0693	0.0566	0.0728	0.0416
GOF	1.054	1.041	1.045	1.017	1.016	1.008
$\Delta\rho_{max}$, $\Delta\rho_{min}$/eÅ^{-3}	1.135, −1.451	0.784, −1.053	0.755, −0.881	0.464, −0.633	0.948, −0.944	0.950, −0.0661

Table 2. Selected geometric parameters (Å, °) for **1**-**5**

Compound **1**			
Mo1-S4	2.1743(13)	Mo1-S1	2.1916(12)
Mo1-S3	2.1827(11)	Mo1-S2	2.2038(11)
S4-Mo1-S3	109.90(5)	S4-Mo1-S2	110.03(5)
S4-Mo1-S1	109.44(5)	S3-Mo1-S2	108.77(4)
S3-Mo1-S1	109.97(5)	S1-Mo1-S2	108.70(5)
Compound **2**			
Mo1-S3	2.1835(6)	Mo1-S1	2.1881(6)
Mo1-S2	2.1878(6)	Mo1-S4	2.1886(7)
S3-Mo1-S2	109.02(3)	S3-Mo1-S4	108.51(3)
S3-Mo1-S1	109.07(3)	S2-Mo1-S4	108.95(3)
S2-Mo1-S1	110.56 (3)	S1-Mo1-S4	110.70(3)
Compound **3**			
Mo1-S3	2.1710(8)	Mo1-S1	2.1935(7)
Mo1-S2	2.1873(7)	Mo1-S4	2.1956(8)
S3-Mo1-S2	109.84(3)	S3-Mo1-S4	109.33(4)
S3-Mo1-S3	109.55(3)	S2-Mo1-S4	109.16(3)
S2-Mo1-S1	109.34(3)	S1-Mo1-S4	109.60(3)
Compound **4**			
Mo1-S1	2.1713(9)	Mo1-S4	2.1804(9)
Mo1-S2	2.1926(9)	Mo1-S3	2.1939(10)
S1-Mo1-S4	109.47(3)	S1-Mo1-S3	108.93(4)
S1-Mo1-S2	108.89(3)	S4-Mo1-S3	111.05(4)
S4-Mo1-S2	108.63(4)	S2-Mo1-S3	109.84(4)
Compound **4-W**			
W1-S1	2.1795(11)	W1-S3	2.2000(12)
W1-S4	2.1907(11)	W1-S2	2.2008(11)
S1-W1-S4	109.45(4)	S1-W1-S2	109.08(4)
S1-W1-S3	109.21(5)	S4-W1-S2	108.40(5)
S4-W1-S3	110.97(5)	S3-W1-S2	109.70(4)
Compound **5**			
Mo1-S2	2.1737(5)	Mo1-S4	2.1864(5)
Mo1-S3	2.1818(5)	Mo1-S1	2.2142(5)
S2-Mo1-S3	109.85(2)	S2-Mo1-S1	110.15(2)
S2-Mo1-S4	108.94(2)	S3-Mo1-S1	109.30(2)
S3-Mo1-S4	108.80(2)	S4-Mo1-S1	109.78(2)

are observed, all of which are shorter than the sum of the van der Waals radii of S and H.[27] The strength, number and nature of these interactions affect the Mo–S bond lengths as exemplified for the longest and the shortest Mo–S bonds: two short N–H···S2 bonds (S2···H: 2.50 and 2.54 Å) with N–H···S2 angles of ≈ 161 °, a bifurcated N–H···S2 contact (S2···H: 2.93 Å, N–H···S2 angle: 114 °) and a C–H···S2 interaction (S···H: 2.90 Å; C–H···S angle: 144.2 °) lead to the long Mo–S2 bond at 2.2038(11) Å. In contrast, for the S4 atom, which has the shortest bond at 2.1743(13) Å to the Mo centre, two bifurcated N–H···S bonds at long distances of 2.81 and 2.89 Å are observed accompanied by N–H···S angles of 146.8 and 116.6 °. Similar analyses of the remaining hydrogen bonding interactions and resulting Mo–S bond lengths show that in general, the Mo–S bond lengths tend to be longer when the S···H contacts are shorter and the N–H···S angles are more obtuse. As a result of the hydrogen bonding interactions the cations and anions are organized such that the ammonium group of the organic cation always points towards the S atoms of the anion leading to a hydrogen bonded chain of $[MoS_4]^{2-}$ along *a* axis (Figure 1).

Along [001] the cations form double-layers which alternate with the anions (Figure 1), while along [010] anions and cations are stacked in a layer like fashion. The volume of the $[MoS_4]^{2-}$ anion was calculated using the minimum bound ellipsoid (MBE) approach and found to be 43.88 Å^3. The shape parameter S of −0.006 indicates a slight axial compression.[32] For gaining more insight into the intermolecular interactions a Hirshfeld surface analysis was performed. In this approach the Hirshfeld surface is mapped over d_{norm}. The quantity d_{norm} is defined according to the following equation (1).

$$d_{norm} = \frac{d_i - r_i^{vdW}}{r_i^{vdW}} + \frac{d_e - r_e^{vdW}}{r_e^{vdW}} \quad (1)$$

In this equation d_i is the distance of a point on the surface to the nearest nucleus inside the surface and d_e is the distance from such a point to the next neighbor outside the surface. The van der Waals radius is abbreviated as vdW. Short distances appear as red areas on the Hirshfeld surface (Figure 2 left), while long distances are colored in green to blue.

In Figure 2, top left, several red areas can be identified caused by intermolecular interactions with distances shorter than the sum of the vdW radii. Because visualization of all contacts is not easy for a 3D object, 2D fingerprint plots are used for a more detailed analysis which is shown in Figure 2 top right for the anion and in the bottom row for the two independent cations. The spike at $d_e/d_i = 0.82/1.42$ Å seen in the fingerprint plot of the anion is caused by S···H interactions (Figure 2, top right). For the two cations two spike-like features are observed which differ from each other. The feature at $d_e/d_i = 1.4/0.8$ Å (Figure 2, bottom left) is due to H···S contacts (37.6 %) and the second at $d_e/d_i = 1.2/1.2$ Å indicates H···H

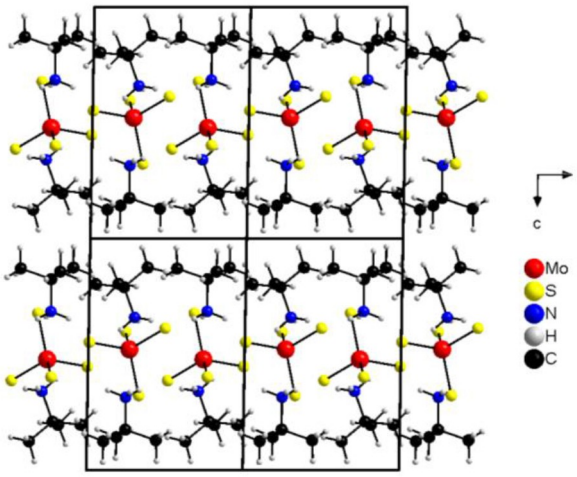

Figure 1. View of the arrangement of the constituents in the structure of compound **1**. For a view of the asymmetric unit see Figure S3.

Table 3. Hydrogen bonding geometry (Å, °) for compounds **1**–**5**.

D–H···A	*D*(D–H) (Å)	*D*(H··A)	*D*(D··A)	< DHA	Symmetry code
Compound **1**					
N1-H1A···S3	0.90	2.39	3.287(4)	173.9	x-1, y, z
N1-H1B···S1	0.90	2.53	3.401(4)	164.3	x, y, z
N1-H1B···S2	0.90	2.93	3.400(4)	114.0	x, y, z
N1-H1C···S2	0.90	2.50	3.361(4)	161.1	−x+1, −y+1, −z+1
C2-H2A···S1	0.97	2.98	3.802(6)	143.8	x, y, z
C3-H3A···S3	0.97	2.94	3.627(6)	128.6	−x+1, −y+1, vz+1
C4-H4C···S1	0.97	2.95	3.772(5)	142.8	x, y, z
N11-H11A···S1	0.90	2.57	3.429(4)	160.6	x, y, z
N11-H11A···S4	0.90	2.89	3.394(3)	116.6	x, y, z
N11-H11B···S2	0.90	2.54	3.407(4)	161.4	−x+1, −y+2, −z+1
N11-H11C···S3	0.90	2.78	3.437(4)	130.6	−x+2, −y+2, −z+1
N11-H11C···S4	0.90	2.81	3.617(4)	150.1	−x+2, −y+2, −z+1
C12-H12C···S1	0.97	2.81	3.662(5)	146.8	x, y, z
C14-H14A···S2	0.97	2.90	3.728(5)	144.2	−x+1, −y+2, −z+1
Compound **2**					
N1-H1N1···S1	0.89	2.67	3.495(2)	155.4	−x+1, −y, −z+1
N1-H2N1···S1	0.89	2.79	3.352(2)	122.5	x, y, z
N1-H2N1···S3	0.89	2.49	3.279(2)	147.5	x, y, z
N1-H3N1···S4	0.89	2.53	3.378(2)	159.8	<M−>x+1/2, −y+1/2, −z+1
C1-H1E···S1	0.97	2.99	3.720(3)	133.1	x+1/2, y+1/2, z
C2-H2A···S2	0.97	2.93	3.533(3)	126.1	−x+1, −y, −z+1
C2-H2B···S4	0.97	2.82	3.669(3)	147.3	−x+1/2, −y+1/2, −z+1
C3-H3A···S3	0.97	2.79	3.710(3)	158.5	−x+1, −y+1, −z+1
C3-H3B···S3	0.97	3.00	3.805(2)	140.7	−x+3/2, −y+1/2, −z+1
N2-H1N2···S2	0.98	2.56	3.342(2)	136.6	−x+3/2, −y+1/2, −z+1
N2-H1N2···S4	0.98	2.88	3.520(2)	123.9	−x+1, −y+1, −z+1
C5-H5A···S2	0.96	2.96	3.809(3)	148.1	x+1/2, −y+1/2, z+1/2
C5-H5B···S3	0.96	2.82	3.736(3)	159.2	x+3/2, −y+1/2, z+1
Compound **3**					
N1-H1N1···S1	0.89	2.59	3.378(3)	147.6	x, y, z
N1-H1N1···S2	0.89	2.81	3.422(2)	126.9	x, y, z
N1-H2N1···S2	0.89	2.56	3.350(2)	148.0	−x+1, −y, −z+1
N1-H2N1···S3	0.89	2.94	3.588(3)	130.9	−x+1, −y, −z+1
N2-H2N2···S1	0.89	2.42	3.306(2)	176.5	x−1/2, −y+1/2, z−1/2
N2-H1N2···S4	0.89	2.47	3.296(3)	153.9	x+1/2, −y+1/2, z−1/2
N2-H1N2···S2	0.89	2.88	3.444(2)	122.7	x+1/2, −y+1/2, z−1/2
Compound **4**					
N1-H1N1···S1	0.91	2.53	3.340(3)	148.7	x, y+1, z
N1-H1N1···S4	0.91	2.88	3.521(3)	128.3	x, y+1, z
N1-H2N1···N4	0.91	1.89	2.795(4)	170.3	−x+1/2, y+1, z−1/2
N1-H3N1···N4	0.91	1.97	2.868(4)	166.8	−x+1/2, y, z−1/2
C1-H1A···S2	0.99	2.91	3.830(3)	155.6	x−1/2, 1−y, z
C1-H1B···S1	0.99	2.64	3.511(3)	146.6	−x+1/2, 1+y, z+1/2,
C2-H2A···S3	0.99	2.94	3.887(4)	159.5	x, y, z
N2-H1N2···S3	0.92	2.90	3.711(3)	147.4	−x+1/2, y, z+1/2
C4-H4A···S2	0.990	2.90	3.515(3)	121.3	x+1, −y+1, z+1/2
C4-H4B···S4	0.99	3.01	3.820	162	x, y, z
N3-H1N3···S2	0.91	2.98	3.536(3)	120.6	−x+1, −y+1, z+1/2
N3-H1N3···S3	0.91	2.53	3.374(3)	155.0	−x+1, −y+1, z+1/2
N3-H2N3···S2	0.91	2.63	3.410(3)	143.7	x, y, z
N3-H2N3···S4	0.91	2.87	3.556(3)	133.8	x, y, z
C5-H5A···S4	0.99	2.87	3.820(4)	162.2	−x+1/2, y, z+1/2
C5-H5B···S3	0.99	2.96	3.789(4)	142.4	x, y, z+1
C6-H6B···S1	0.99	2.96	3.692(4)	132.0	x, y, z+1
N4-H1N4···S2	0.92	2.75	3.601(3)	154.9	x, y, z
N4-H2N4···S1	0.92	2.69	3.357(3)	130.3	−x+1, −y, z+1/2
N4-H2N4···S2	0.92	2.95	3.783(3)	150.8	−x+1, −y, z+1/2
Compound **5**					
N1-H1···S4	1.00	2.29	3.2551(17)	162.5	x, y, z

Table 3. continued

D–H···A	*D*(D–H) (Å)	*D*(H··A)	*D*(D··A)	< DHA	Symmetry code
N2-H2C··· O1	0.91	1.99	2.8979(19)	174.0	x+1/2, y+1/2, z
N2-H2D···S1	0.91	2.54	3.3180(18)	143.3	−x+3/2, −y+1/2, z+1
N2-H2D···S3	0.91	2.76	3.3278(17)	121.1	−x+3/2, −y+1/2, z+1
C1-H1A···S1	0.99	2.91	3.803(2)	150.4	−x+3/2, y+1/2,−z+3/2
C1-H1B···S3	0.99	3.01	3.9302(19)	155.0	−x+1, −y+1, −z+1
C2-H2A···S4	0.99	2.86	3.656(2)	138.4	x, y, z
C2-H2B···S2	0.99	2.87	3.598(2)	130.9	x+1/2, y+1/2, z
C2-H2B···S3	0.99	2.77	3.5730(19)	138.2	x+1/2, y+1/2, z
C3-H3B···S1	0.99	2.97	3.631(2)	125.3	x, y, z
C3-H3B···S4	0.99	3.01	3.759(2)	133.1	x, y, z
C4-H4B···S3	0.99	2.86	3.551(2)	127.3	x+1/2, −y+1/2, z+1/2
C5-H5A···S2	0.98	2.94	3.851(2)	154.9	−x+1, y, −z+3/2
C5-H5B···S4	0.98	2.87	3.588(2)	131.2	−x+1, −y+1, −z+1
C5-H5C···S1	0.98	2.88	3.769(2)	151.7	−x+3/2, y+1/2,−z+3/2
O1-H101···S1	0.84	2.55	3.3361(9)	155.6	x, y, z
O1-H101···S2	0.84	2.94	3.4652(18)	122.2	x, y, z

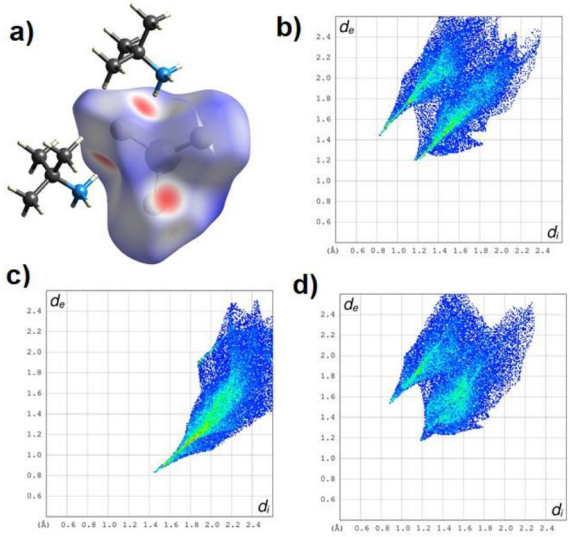

Figure 2. Top left: The Hirshfeld surface of the anion in the structure of **1**; top right: the fingerprint plot for the anion; bottom left: the fingerprint plot of cation 1 (N1) and bottom right of cation 2 (N11).

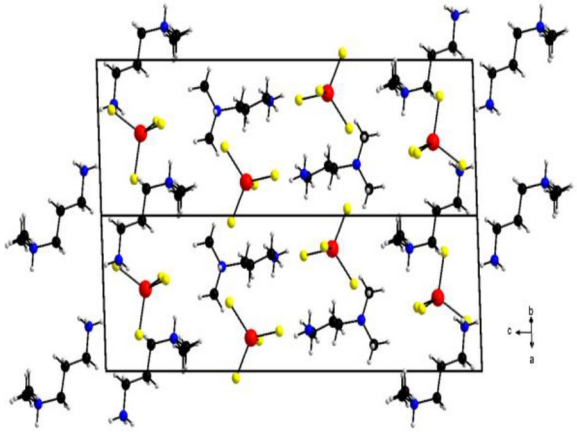

Figure 3. View of the arrangement of the constituents in the structure of **2** viewed along [110]. (For the asymmetric unit of **2** see Figure S4) The colour code is identical with that shown in Figure 1.

interactions (62.4%). For the second cation (Figure 2 bottom right) the spike $d_e/d_i = 1.5/0.9$ Å is caused by H···S interactions (33.1%) while that located at 1.2/1.2 Å is due to H···H contacts (66.9%).

The structure of **2** consists of a diprotonated N^1,N^1-dimethyl-propane-1,3-diamine and a $[MoS_4]^{2-}$ anion (Figure 3) with all atoms located in general positions. The MoS_4 tetrahedron is slightly distorted with S–Mo–S angles between 108.51(3) and 110.70(3) (Table 2). In contrast to **1**, the Mo–S bond lengths scatter in a very narrow range between 2.1835(6) and 2.1886(7) Å with an average Mo–S distance of 2.1870 Å. The volume of the $[MoS_4]^{2-}$ anion of 43.80 Å^3 does not significantly differ from that of compound **1**. But the shape parameter S = 0.006 indicates a small axial elongation. Three of the Mo–S distances are indistinguishable within experimental error and the difference Δ is 0.0051 Å, clearly much lower than for **1**. Like in **1** the cations and anions are involved in two types of hydrogen bonding interactions. Each anion is hydrogen bonded to seven cations *via* six N–H···S and seven C–H···S bonds and *vice versa* (Figure S6, Table 3). The S1, S2 and S4 atoms each have three hydrogen bonding contacts while S3 has four S···H bonds. The S···H separations as well as the N/C–H···S angles indicate different strengths of the bonds. The cations and anions alternate along [010] and [001] to form a rod-like arrangement. As a result of hydrogen bonding, the cations and anions are organized into a 3D network.

The Hirshfeld surface of the anion (Figure 4, top) shows several red areas indicative of interionic interactions, which can be clearly seen as S···H contacts in the fingerprint plot (Figure 4, bottom left). It should be noted that the d_e/d_i values slightly differ from that observed in the fingerprint plot of the anion of compound **1**. The shape of the fingerprint plot of the cation (Figure 4, bottom right) shows a spike at $d_e/d_i = 1.4/0.8$ Å

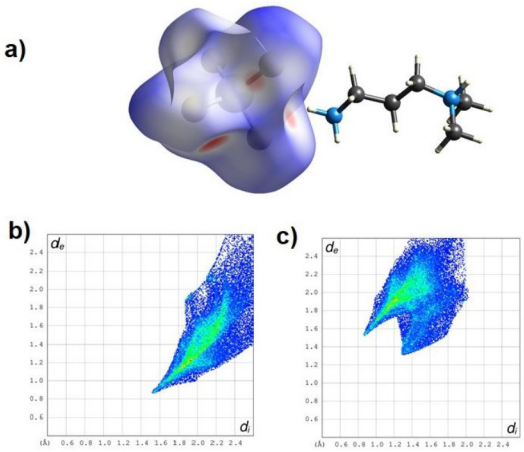

Figure 4. Top: The Hirshfeld surface of the anion in the structure of **2**; bottom left: the fingerprint plot for the anion; bottom right: the fingerprint plot for the cation.

representing H···S contacts (61.8%) while that at $d_e/d_i = 1.3/1.3$ is caused by H···H interactions (38.2%).

Compound **3** is isostructural with the corresponding W analogue[23] and crystallizes in the monoclinic space group $P2_1/n$ with all atoms located in general positions. The substitution of W by Mo in **3** results in a slightly reduced unit cell volume of 1295.29(14) Å^3 (cell volume of W compound: 1311.5(2) Å^3). The structure consists of a diprotonated *N,N′*-dimethylpropane-1,3-diamine molecule and a $[MoS_4]^{2-}$ anion (Figure 5). The S–Mo–S angles are close to the ideal value and range between 109.16 (3) and 109.84 (3) ° (Table 2). The Mo–S bond lengths vary from 2.1710 (8) to 2.1956 (8) Å (average: 2.1868 Å), and the Δ value of 0.0246 Å is slightly longer than that observed for **2** and comparable with the value calculated for **1**. The volume of the tetrahedron is 43.81 Å^3 with a shape parameter S = 0.0005 indicating a very small distortion of the polyhedron. Unlike the W compound, the C2 and C3 atoms in the cation in **3** are disordered over two positions and were refined using a split model. The H atoms attached to C4 are also disordered.

Due to this disorder a detailed discussion of C–H···S bonding in **3** is not possible. In the structure each anion is surrounded by four cations and is involved in a total of seven N–H···S interactions (Table 3). Along [010] and [001] cations and anions alternate and along [100] the cations and anions occur pairwise.

Compound **4** crystallizes in the non-centrosymmetric orthorhombic space group $Pca2_1$. Its structure consists of a crystallographically independent 2-amino-N-{2-[(2-ammonio-ethyl) amino]ethyl}ethaneminium cation $(trienH_2)^{2+}$ (Scheme 2) and a unique $[MoS_4]^{2-}$ anion with all atoms located in general positions (Figure 6).

In the structure the anions appear as pairs along [100] separated by pairs of cations, and along [010] and [001] the $[MoS_4]^{2-}$ anions are arranged in a zig-zag-like manner (Figure 6, top). Another structure of a $[MoS_4]^{2-}$ compound with this cation was reported by Pokrel et al.[33] (CCDC Refcode EVIREG,). However, in this structure both terminal N atoms are protonated and the cation is 2,2′-(ethane-1,2-diylbis(azaanediyl)) diethanaminium (See Scheme 2). The compound crystallized also in the non-centrosymmetric orthorhombic space group

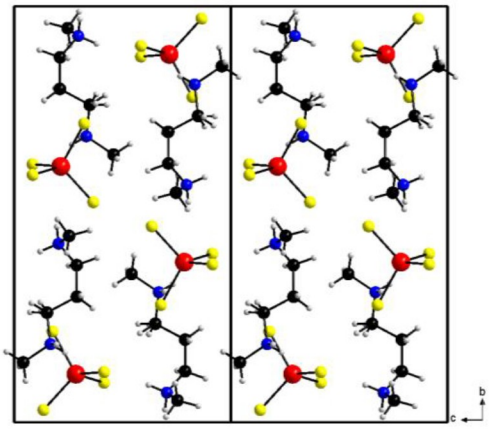

Figure 5. View of the arrangement of the anions and cations in the structure of compound **3**. (For the asymmetric unit of **3** see Figure S4) Disordered atoms are not shown and the colour code is identical with that in Figure 1.

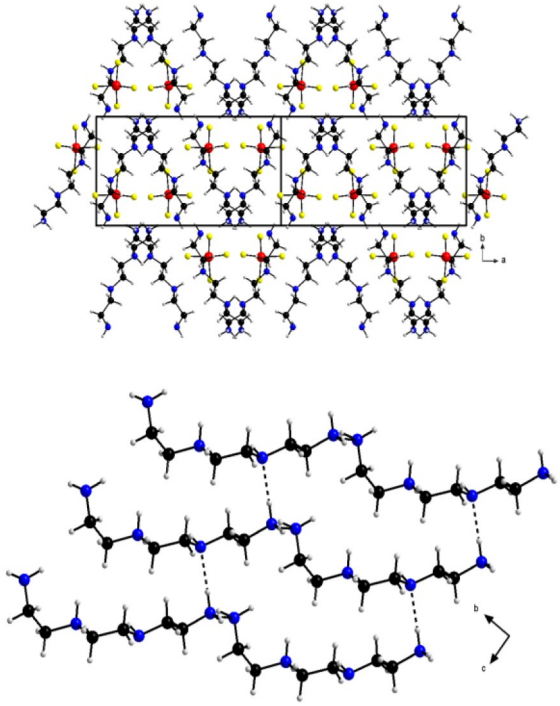

Figure 6. A view of the arrangement of the cations and anions in the structure of compound **4** viewed along [001] (**top**) (For the asymmetric unit of **4** see Figure S5). The hydrogen bonds (broken lines) between the cations in the structure of **4** viewed along [100] (**bottom**). The colour code is identical with that in Figure 1.

*Pca*2$_1$ with a large unit cell volume (2953.45 Å^3) and comprises two unique cations and two unique anions. In the dication in **4**, a terminal amine N and an inner N atom are protonated. We characterized the W analogue with the cation as in **4** (**4-W**) which adds credence to our results (Figure S7). The geometric parameters of the $[MoS_4]^{2-}$ tetrahedron indicate a moderate distortion (S–Mo–S angles: 108.63(4) - 111.05(4)°) with Mo–S bond lengths ranging from 2.1713(9) to 2.1939(10) Å (Table 2) (< Mo–S >: 2.1820 Å; $\Delta = 0.0226$ Å). A similar distortion of the $[WS_4]^{2-}$ tetrahedron is observed for **4-W**. The volume of the $[MoS_4]^{2-}$ tetrahedron is 43.65 Å^3 and the shape parameter S of 0.013 indicates an axial elongation. All N–H hydrogen and some C–H hydrogen atoms (C1, C2, C4, C5 and C6) act as hydrogen donors while all the four S atoms and the N2 and N4 atoms function as hydrogen acceptors resulting in a total of twenty hydrogen bonds (Table 3) of which two are N–H···N interactions (Figure 6, bottom). The latter generate a layer-like network of interconnected cations in **4** and **4-W** (Figure S7). The $[MoS_4]^{2-}$ moiety is linked with eight symmetry related cations with the aid of N–H···S and C–H···S interactions, while the cation is connected with two symmetry related cations and eight $[MoS_4]^{2-}$ units (Figure S8). The S3 atom is associated with the shortest S···H contact (Table 3) and therefore has the longest bond to Mo at 2.1939(7) Å. The other distinct Mo–S distances can be similarly explained due to the strength and number of S···H interactions. The net result of hydrogen bonding is organisation of organic dications and anions into alternating layers.

The Hirshfeld surface of both the anion and cation show several red areas indicative of strong H bonding interactions (Figure 7, top). The spike observed at $d_e/d_i = 0.9/1.5$ Å (Figure 7, bottom left) is caused by the S···H interactions. For the cation the fingerprint plot exhibits four pronounced spikes with the H···S interactions located at $d_e/d_i = 1.55/0.9$ Å (42.1 %), H···N at $d_e/d_i = 1.1/0.7$ Å (3.7 %), N···H at $d_e/d_i = 1.1/0.7$ Å (3.8 %), and the remaining feature at $d_e/d_i = 1.1/1.1$ Å are H···H interactions (49.9 %).

Compound **5** $(C_5H_{14}N_2)[MoS_4]\cdot{}^1/_2H_2O$ crystallizes in the centrosymmetric monoclinic space group *C2/c* and the structure is composed of a 1-methylpiperazinediium dication and a tetrahedral $[MoS_4]^{2-}$ dianion located in general position and a lattice water molecule with the oxygen atom situated on a twofold rotation axis (Figure 8). In the structure the cations form strands along [001] and in the adjacent strand anions and crystal water molecules alternate in this direction (Figure 8). Along the a-axis these different strands alternate (Figure 8). It is interesting to note that compound **5** is structurally more similar to the earlier reported $(C_6H_{17}N_3)[MoS_4]\cdot{}^1/_2H_2O$[30] ($C_6H_{17}N_3$ = 4-(2-ammonioethyl)-piperazin-1-ium) which also crystallizes in *C2/c* and not to its corresponding W analogue.[34] The tetrasulfidometallates of Mo and W charge balanced by the 1-methylpiperazinediium cation contain different amounts of crystal water molecules and the monohydrated W analog $(C_5H_{14}N_2)[WS_4]\cdot H_2O$ crystallizes in the centrosymmetric monoclinic space group $P2_1/c$.[34] The cyclic diamine adopts a chair confirmation with the methyl group occupying the equatorial position (Figure 8). The geometric parameters of the $[MoS_4]^{2-}$ tetrahedron indicate a slight distortion (S–Mo–S angles: 108.80(2) - 110.15(2) °) with Mo–S bond lengths varying from 2.1737(5) to 2.2142(5) Å (average: 2.1890 Å; Table 2). The observed geometric parameters are in very good agreement with other $[MoS_4]^{2-}$ compounds charge balanced by cations based on piperazine.[21,30, 35] The value for Δ of 0.0405 Å is comparable with that observed in other tetrasulfidomolybdates charge balanced by organic cations based on piperazine. In **5**, three of the Mo–S bonds are shorter than the average Mo–S bond length while one Mo–S bond is longer at 2.2142(5) Å. The volume of the anion is 43.93 Å^3 and the shape parameter S = 0.009 shows a slight axial elongation. The Mo–S bonding pattern can be again attributed to intermolecular interactions among the organic cation, $[MoS_4]^{2-}$ anion and lattice water. In the structure, eight hydrogen bond donors, namely two

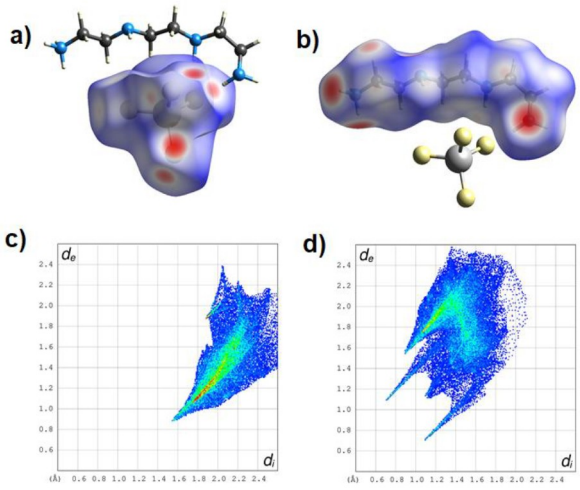

Figure 7. top: Hirshfeld surfaces of the anion (left) and of the cation (right) of compound **4**. Bottom: the corresponding fingerprint plots.

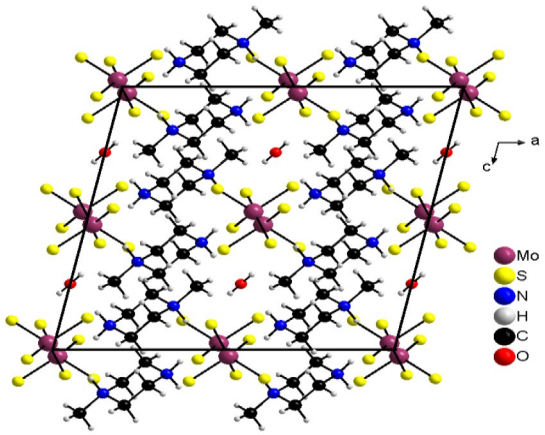

Figure 8. View of the arrangement of anions, cations and water molecules in the structure of **5**. (For the asymmetric unit of **5** see Figure S5).

ammonium groups, four methylene groups, a methyl group and a crystal water molecule, and two hydrogen acceptors viz. tetrasulfidotungstate and crystal water are observed. The $[MoS_4]^{2-}$ anion provides four acceptor sites and thus the entire molecular surface is decorated with hydrogen bond donors and acceptors. The organic cation, $[MoS_4]^{2-}$ and H_2O are linked with the aid of four varieties of H-bonding interactions: three N–H···S, one N–H···O, two O–H···S, and eleven C–H···S bonds (Table 3). The H_2O molecule has O–H···S bonds to two symmetry related $[MoS_4]^{2-}$ anions while the O atom of H_2O functions as hydrogen acceptor in N–H···O interactions to two cations (Figure S9). Each $[MoS_4]^{2-}$ unit is linked to six different cations and a H_2O molecule via N–H···S, C–H···S and O–H···S interactions, while the cation is hydrogen bonded to seven different $[MoS_4]^{2-}$ anions and a H_2O via three N–H···S, nine C H···S and one N–H···O interaction (Figure S10). The longest Mo–S1 bond can be explained due to a total of four weak interactions viz. a N–H···S bond, two C–H···S bonds (2.88, 2.91 Å) and a short O–H···S bond at 2.55 Å (Table 3), while the shortest Mo–S2 bond is accompanied by two C–H···S contacts (2.87, 2.94 Å) and a weak O–H···S bond (2.94 Å) but no N–H···S interaction. As a result of the four varieties of hydrogen bonding interactions in **5**, the organic cation, $[MoS_4]^{2-}$ anion and the lattice water molecule are organized into an intricate three-dimensional network (Figure S11).

The Hirshfeld surfaces of the anion and cation are displayed in Figure 9 in the top row. Like for the other compounds discussed above several red areas on the surfaces evidence short intermolecular contacts. In the fingerprint plot of the anion (Figure 9, bottom left) the spike at $d_e/d_i \approx 0.82/1.42$ Å are related to S···H interactions. For the cation (Figure 9, bottom right) three special features are observed at $d_e/d_i \approx 1.42/10.82$, at $d_e/d_i \approx 1.1//0.78$, and at $d_e/d_i \approx 1.28/1.28$ Å which are caused by H···S, H···O, and H···H interactions, respectively.

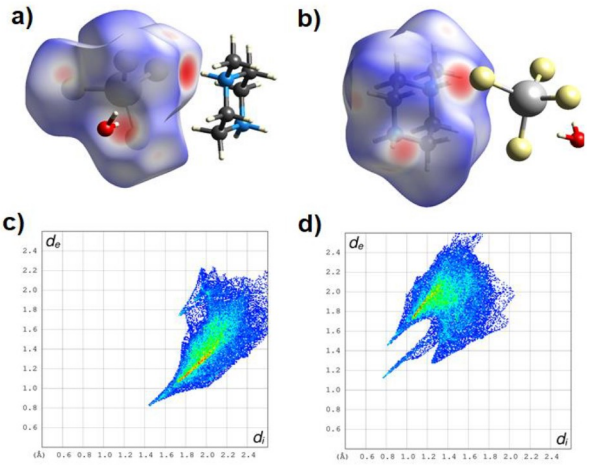

Figure 9. top: The Hirshfeld surface of the anion (left) and of the cation (right); bottom: the fingerprint plots for the anion (left) and for the cation (right) in the structure of **5**.

2.4. Structural chemistry of tetrasulfidomolybdates

A survey of the Cambridge Structural Database (CSD)[36] reveals more than thirty tetrasulfidomolybdates have been structurally characterized (Table 4).[21,25,26,30,33,35,37–55] The availability of structural information of several compounds permits a comparative study, the details of which are described here. The isolation of $[MoS_4]^{2-}$ anions charge balanced by a variety of cations namely alkali metal cations like K^+, Rb^+, Cs^+, (entry nos. 1-3) metal-organic cations (entry nos. 35-37) like $[Co_2(tren)_3]^{2+}$ (tren = tris (2-aminoethylamine) $[Mn(dien)_2]^{2+}$ (dien = diethylenetriamine) $[Ni(en)_3]^{2+}$ (en = ethylenediamine), organic ammonium cations (entry nos. 5-34) indicates the flexibility of the non-centrosymmetric $[MoS_4]^{2-}$ tetrahedron to exist in different structural environments. The first twenty-four compounds listed in Table 4 crystallize in centrosymmetric space groups, while the remaining (~37%) are observed in non-centrosymmetric structures. Although most of the compounds are crystallized from aqueous solutions, only three are reported to contain crystal water molecules, namely $(C_6H_{17}N_3)[MoS_4]\cdot{}^1/_2H_2O$, $(trenH_2)[MoS_4]\cdot H_2O$ and compound **5**. For each $[MoS_4]^{2-}$ compound in Table 4, the corresponding isostructural W analog has been characterized, excepting in the case of compound **5** which is a hemihydrate while the known W analog containing the same 1-methylpiperazine-1,4-diium cation is a monohydrate which crystallizes in the monoclinic $P2_1/c$ space group. In many compounds the N atoms are fully protonated. However, it is noted that in some cases, especially the compounds isolated from the base promoted cation exchange reactions by using tri-, or tetraamines, the cations are partially protonated. In the case of some amine molecules like tren, dipn, trien etc. there is more than one structural possibility of a dication (Scheme S2).

The tetrasulfidomolybdate compounds of the alkali metal (K^+, Rb^+, Cs^+), ammonium, methylammonium are isostructural and crystallize in the centrosymmetric *Pnma* space group. The compounds containing metal-organic cations for charge compensation crystallize in non-centrosymmetric space groups. Excepting $[Mn(dien)_2][MoS_4]$ which shows four identical Mo–S bonds, in all other compounds the $\{MoS_4\}$ tetrahedron is slightly distorted, which can be attributed to the cation-anion interactions. For all the compounds the longest Mo–S bond distance varies from 2.2142 (observed in compound **5**) to 2.1765 Å. In our work we have defined the difference Δ between the longest and shortest Mo–S bond lengths as a measure of distortion of the $\{MoS_4\}$ tetrahedron and a maximum value of 0.0431 Å was observed for the $[MoS_4]^{2-}$ compound charge balanced by the diprotonated cation of piperazine[21] and the Δ value for **5** (0.0405 Å) which exhibits the longest Mo–S distance is very close.

Organic ammonium tetrasulfidomolybdates charge balanced by tetra-alkylated organic cations exhibit only C–H···S interactions while all other organic ammonium compounds exhibit a minimum of two types of interactions, namely N–H···S and C–H···S interactions. Compounds with an unprotonated N atom in the organic cation (see entry nos. 9, 13, 23, 27, 28) exhibit N–H···N interactions as observed in compound **3**, in

Table 4. Structural features of tetrasulfidomolybdates.

No.	Compound	Space Group	Mo-S (long) Å	Δ (Å)	Secondary Interaction	Ref
1	$K_2[MoS_4]$	*Pnma*	2.2000	0.0243	K···S	37
2	$Rb_2[MoS_4]$	*Pnma*	2.1917	0.0135	Rb···S	38
3	$Cs_2[MoS_4]$	*Pnma*	2.1935	0.0126	Cs···S	39
4	$(NH_4)_2[MoS_4]$	*Pnma*	2.186	0.015	N–H···S	40
5	$(PrNH_3)_2[MoS_4]$[a]	*Pnma*	2.1876	0.0043	N–H···S	41
6	$(CH_3\text{-}NH_3)_2[MoS_4]$	*Pnma*	2.1961	0.0199	N–H···S, C–H···S	42
7	$[(Pr)_4N]_2[MoS_4]$	*C2/c*	2.1928	0.0179	C–H···S	21
8	$(mipaH)_2[MoS_4]$	*C2/c*	2.2085	0.0390	N–H···S, C–H···S	43
9	$(trans\text{-}1,2\text{-}cnH)_2[MoS_4]$	*C2/c*	2.1876	0.0125	N–H···S, C–H···S, N–H···N	44
10	$(C_5H_{16}N_2)[MoS_4]$ **2**	*C2/c*	2.1886	0.0051	N–H···S, C–H···S	This work
11	$(Me\text{-}pipH_2)[MoS_4]\cdot{}^1/_2H_2O$ **5**	*C2/c*	2.2142	0.0405	N–H···S, C–H···S, N–H···O, O–H···S	This work
12	$(C_6H_{17}N_3)[MoS_4]\cdot{}^1/_2H_2O$	*C2/c*	2.2005	0.0302	N–H···S, C–H···S, N–H···O, O–H···S	30
13	$(trenH_2)[MoS_4]\cdot H_2O$	$P2_1/c$	2.1951	0.0281	N–H···S, C–H···S, N–H···N, N–H···O, O–H···S	21
14	$(1,3\text{-}pnH_2)[MoS_4]$	$P2_1/c$	2.1882	0.0183	N–H···S, C–H···S	45
15	$(pipH_2)[MoS_4]$	$P2_1/c$	2.2114	0.0431	N–H···S, C–H···S	21
16	$(tmenH_2)[MoS_4]$	$P2_1/n$	2.1983	0.0289	N–H···S, C–H···S	45
17	$[(CH_3)_2NH_2]_2[MoS_4]$	$P2_1/n$	2.2176	0.0354	N–H···S, C–H···S	46
18	$(C_5H_{16}N_2)[MoS_4]$[a] **3**	$P2_1/n$	2.1956	0.0246	N–H···S	This work
19	$[(Et)_4N]_2[MoS_4]$[b]	*Pī*	2.187	0.016	C–H···S	47
20	$(1,4\text{-}bnH_2)[MoS_4]$	*Pī*	2.1992	0.0243	N–H···S, C–H···S	48
21	$(trans\text{-}1,4\text{-}cnH)_2[MoS_4]$	*Pī*	2.1955	0.0181	N–H···S, C–H···S	44
22	$[(PhCH_2)(CH_3)NH_2]_2[MoS_4]$	*Pī*	2.1908	0.0326	N–H···S, C–H···S	49
23	$(pipH)_2[MoS_4]$	*Pī*	2.2115	0.0381	N–H···S, C–H···S, N–H···N	35
24	$(C_4H_{12}N)_2[MoS4]$ **1**	*Pī*	2.2038	0.0295	N–H···S, C–H···S	This work
25	$(dabcoH)(NH_4)[MoS_4]$	$P2_13$	2.1854	0.0092	N–H···S, C–H···S	50
26	$(trienH_2)[MoS_4]$[b]	$Pca2_1$	2.200	0.027	N–H···S, C–H···S	33
27	$(C_6H_{20}N_4)[MoS_4]$ **4**	$Pca2_1$	2.1939	0.0226	N–H···S, C–H···S, N–H···N	This work
28	$(dipnH_2)[MoS_4]$	$Pca2_1$	2.1903	0.0186	N–H···S, C–H···S, N–H···N,	30
29	$[(Me)_4N]_2[MoS_4]$[a, c]	$P2_12_12_1$	2.177	0.018	–	51
30	$(enH_2)[MoS_4]$	$P2_12_12_1$	2.1846	0.0111	N–H···S, C–H···S	52
31	$(Me\text{-}enH_2)[MoS_4]$	$P2_12_12_1$	2.2014	0.0379	N–H···S, C–H···S	31
32	$R\text{-}[PhCH(Me)NH_3]_2[MoS_4]$	$P2_1$	2.2066	0.0422	N–H···S, C–H···S	53
33	$S\text{-}[PhCH(Me)NH_3]_2[MoS_4]$	$P2_1$	2.2056	0.0401	N–H···S, C–H···S	53
34	$[(Bu)_4N]_2[MoS_4]$	*Fdd2*	2.2047	0.0255	C–H···S	51
35	$[Co_2(tren)_3][MoS_4]_2$	*Fdd2*	2.1901	0.0270	N–H···S, C–H···S	25
36	$[Ni(en)_3][MoS_4]$	$Pna2_1$	2.1865	0.0099	N–H···S, C–H···S	54
37	$[Mn(dien)_2][MoS_4]$	*I*-4	2.1765	0	N–H···S, C–H···S	26
38	$(NH_4)_6[MoS_4]_3\cdot(hmt)_4$	*R3c*	2.2122	0.0368	N–H···S, C–H···S	55

Abbreviations used: Δ = Difference between the longest and shortest Mo-S bond distance; [a] Disordered cations; [b] Two crystalllographically independent $[MoS_4]^{2-}$ units; [c] Three crystalllographically unique $[MoS_4]^{2-}$ ions; for compounds with more than one unique $[MoS_4]^{2-}$ unit the parameters are listed for the unit which shows maximum Δ. $PrNH_3$ = n-propylammonium; Pr = n-propyl; mipa = monoisoprop-ylamine; trans-1,2-cn = (±)trans-1,2-cyclohexanediamine; $(C_6H_{17}N_3)$ = 4-(2-ammonioethyl)-piperazin-1-ium; Me-$pipH_2$ = 1-methylpiperazinediium $pipH_2$ = piperazinediium; 1,3-pn = propane-1,3-diamine; tren = tris(2-aminoethyl)amine; Et = ethyl; tmen = N,N,N′,N′-tetramethylethylenediamine; 1,4-bn = butane-1,4-diamine; trans-1,4-cn = trans-1,4-cyclohexanediamine; pipH = piperazin-1-ium; dabco = diazabicyclononane; trien = triethylenetetramine; dipn = dipropylenetriamine; Me = methyl; en = ethylenediamine; Me-en = N-methylethylenediamine; Bu = n-butyl; dien = diethylenetriamine, hmt = hexamethylenetetramine

addition to N–H···S and C–H···S. Hydrated organic ammonium tetrasulfidomolybdates (entry nos. 11-13) exhibit four varieties of interactions as observed in compound **5**.

3. Conclusions

In summary, the synthesis, spectra and structures of five new organic ammonium tetrasulfidomolybdates are described. The compounds (**1**) to (**5**) described in this work constitute five new examples to the growing list of structurally characterized organic ammonium tetrasulfidomolybdates. A detailed analysis of the crystal structures reveals extensive hydrogen bonding interactions between the organic cation and the $[MoS_4]^{2-}$ anion resulting in a distortion of the $\{MoS_4\}$ tetrahedron as evidenced by distinct Mo–S bond distances. The determination of the shape parameter confirms that the $\{MoS_4\}$ tetrahedron exhibits an axial compression in **1** and axial elongation in **2**, **4** and **5** respectively. The Hirshfeld surface analyses demonstrate the existence of intermolecular S···H interactions between the anions and cations. These analyses also show that intermolecular H···H contacts should not be ignored because these interactions contribute to the overall arrangement of the structural constituents. A comparative study of thirty-eight $[MoS_4]^{2-}$ compounds reveals a rich and variable structural chemistry of this group of compounds.

Supporting Information Summary

Deposition Numbers (722294 (**1**), 722295 (**2**), 722296 (**3**), 722293 (**4**) 722292 (**4-W**) 748314 (**5**), contain the supplementary crystallographic data of the compounds described in this paper. These data are provided free of charge by the joint Cambridge Crystallographic Data Centre and Fachinformationszentrum Karlsruhe Access Structures service www.ccdc.cam.ac.uk/structures. Supplementary information of the synthesis procedures, schemes (Scheme S1-S2), results of chemical analyses, experimental details, representative IR and UV-vis spectra and supplementary Figures (Figures S1-S11) associated with this article are available online.

Acknowledgements

BRS acknowledges the University Grants Commission (UGC), New Delhi for financial support to the School of Chemical Sciences (formerly Department of Chemistry), at the level of DSA-I under the Special Assistance Program (SAP). WB acknowledges financial support by the State of Schleswig-Holstein.

Conflict of Interest

The authors declare no conflict of interest.

Keywords: Crystal structure · Hirshfeld analysis · H-bonding interactions · Organic tetrasulfidomolybdate

[1] G. Krüss, *Justus Liebigs Ann. Chem.* **1884**, *225*, 1–57.
[2] G. Brauer, *Handbook of Preparative Inorganic Chemistry*, Volume 2 (2nd Ed) Academic Press **1965**, 1416.
[3] E. Diemann, A. Müller, *Coord. Chem. Rev*. **1973**, *10*, 79–122 and references therein.
[4] A. Müller, E. Diemann, R. Jostes, H. Bögge, *Angew. Chem., Int. Ed. Engl.* **1981**, *20*, 934–955 and references therein.
[5] T. Shibhahara, *Coord. Chem. Rev.* **1993**, *123*, 73–147.
[6] S. H. Laurie, *Eur. J. Inorg. Chem.* **2000**, 2443–2450.
[7] B. R. Srinivasan, S. N. Dhuri, A. R. Naik, *Tetrahedron Lett.* **2004**, *45*, 2247–2249.
[8] S. E. Skrabalak, K. E. Suslick, *J. Am. Chem. Soc.* **2005**, *127*, 9990–9991.
[9] G. J. Brewer, *Drug Discovery Today* **2005**, *10*, 1103–1109.
[10] M. Poisot, W. Bensch, S. Fuentes, C. Ornelas, G. Alonso, *Catal. Lett.* **2007**, *117*, 43–52.
[11] M. Polyakov, M. Poisot, W. Bensch, M. Muhler, W. Grünert, *J. Catal.* **2008**, *256*, 137–144.
[12] C. J. Crossland, I. R. Evans, J. S. O. Evans, *Dalton Trans* **2008**, 1597–1601.
[13] H. J. Jakobsen, H. Bildsoe, J. Skibsted, M. R. Hansen, M. Brorson, B. R. Srinivasan, W. Bensch, *Inorg. Chem.* **2009**, *48*, 1787–1789.
[14] H. J. Jakobsen, H. Bildsøe, J. Skibsted, M. Brorson, B. R. Srinivasan, C. Näther, W. Bensch, *Phys. Chem. Chem. Phys.* **2009**, *11*, 6981–6986.
[15] C. Venkateswarlu, V. Gautam, S. Chandrasekaran, *Carbohydrate Research* **2015**, *402*, 200–207.
[16] S. Mangelsen, B. R. Srinivasan, U. Schürmann, L. Kienle, C. Näther, W. Bensch, *Dalton Trans.* **2019**, *48*, 1184–1201.
[17] D. K. Langlois, J. R. Querubin, W. D. Schall, N. C. Nelson, R. C. Smedley, *Journal of Veterinary Internal Medicine* **2019**, *33*, 1336–1343.
[18] B. K. Maiti, J. J. G. Moura, *Coord. Chem. Rev.* **2021**, *429*, 213635.
[19] X. Wu, W. Zhong, H. Ma, X. Hong, J. Fan, H. Yu, *Journal of Colloid and Interface Science* **2021**, *586*, 719–729.
[20] B. R. Srinivasan, S. N. Dhuri, C. Näther, W. Bensch, *Inorg. Chim. Acta* **2005**, *358*, 279–287.
[21] B. R. Srinivasan, S. N. Dhuri, M. Poisot, C. Näther, W. Bensch, *Z. Naturforsch.* **2004**, *59b*, 1083–1092.
[22] B. R. Srinivasan, S. N. Dhuri, M. Poisot, C. Näther, W. Bensch, *Z. Anorg. Allg. Chem.* **2005**, *631*, 1087–1094.
[23] B. R. Srinivasan, C. Näther, S. N. Dhuri, W. Bensch, *Monatsh. Chem.* **2006**, *137*, 397–411.
[24] B. R. Srinivasan, C. Näther, S. N. Dhuri, W. Bensch, *Polyhedron* **2006**, *25*, 3269–3277.
[25] J. Ellermeier, W. Bensch, *Z. Naturforsch.* **2001**, *56b*, 611–619.
[26] J. Ellermeier, W. Bensch, *Monatsh. Chem.* **2002**, *133*, 945–957.
[27] A. Bondi, *J. Phys. Chem.* **1964**, *68*, 441–451.
[28] J. W. McDonald, G. D. Friesen, L. D. Rosenhein, W. E. Newton, *Inorg. Chim. Acta* **1983**, *72*, 205–210.
[29] K. Nakamoto , *Infrared and Raman Spectra of Inorganic and Coordination Compounds (Part A)*, Sixth ed., John Wiley, New Jersey, **2009**, 194.
[30] B. R. Srinivasan, S. N. Dhuri, A. R. Naik, C. Näther, W. Bensch, *Polyhedron* **2008**, *27*, 25–34.
[31] G. M. Sheldrick, *Acta Crystallogr.* **2015**, *C71*, 3–8.
[32] J. Cumby, P. Attfield, *Nature Commun.* **2016**, *8*, 14235.
[33] S. Pokhrel, K. S. Nagaraja, B. Varghese, *J. Struc. Chem.* **2003**, *44*, 689–694.
[34] B. R. Srinivasan, A. R. Naik, C. Näther, W. Bensch, *Indian J. Chem.* **2010**, *49 A*, 437–441.
[35] B. R. Srinivasan, A. R. Naik, M. Poisot, C. Näther, W. Bensch, *Polyhedron* **2009**, *28*, 1379–1385.
[36] C. R. Groom, I. J. Bruno, M. P. Lightfoot, S. C. Ward, *Acta Crystallogr.* **2016**, *B72*, 171–179.
[37] M. Emirdag-Eanes, J. A. Ibers, *Z. Kristallogr New Cryst. Struct.* **2001**, *216*, 484.
[38] J. Ellermeier, C. Näther, W. Bensch, *Acta Crystallogr.* **1999**, *C55*, 1748–1751.
[39] C. C. Raymond, P. K. Dorhout, S. M. Miller, *Z Kristallogr.* **1995**, *210*, 775–775.
[40] P. J. Lapasset, N. Chezeu, P. Belougne, *Acta Crystallogr.* **1976**, *B32*, 3087–3088.
[41] B. R. Srinivasan, C. Näther, A. R. Naik, W. Bensch, *Acta Crystallogr.* **2006**, *E62*, m1635-m1627.
[42] B. R. Srinivasan, A. R. Naik, C. Näther, W. Bensch, *Indian J. Chem.* **2009**, *48 A*, 769.
[43] B. R. Srinivasan, C. Näther, A. R. Naik, W. Bensch, *Acta Crystallogr.* **2008**, *E64*, m66–m67.
[44] B. R. Srinivasan, C. Näther, W. Bensch, *Acta Crystallogr.* **2006**, *C62*, m98-m101.
[45] B. R. Srinivasan, S. N. Dhuri, C. Näther, W. Bensch, *Inorg. Chim. Acta* **2005**, *358*, 279–287.
[46] B. R. Srinivasan, S. V. Girkar, C. Näther, W. Bensch, *J. Coord. Chem.* **2009**, *62*, 3559–3572.
[47] M. G. Kanatzidis, D. Coucouvanis, *Acta Crystallogr.* **1983**, *C39*, 835–838.
[48] B. R. Srinivasan, C. Näther, W. Bensch, *Acta Crystallogr.* **2005**, *E61*, m2454-m2456.
[49] B. R. Srinivasan, S. V. Girkar, P. Raghavaiah, *Acta Crystallogr.* **2007**, *E63*, m2737-m2738.
[50] S. Pokhrel, K. S. Nagaraja, B. Varghese, *J. Struc. Chem.* **2003**, *44*, 900–905.
[51] M. Poisot, C. Näther, W. Bensch, *Z. Naturforsch.* **2007**, *62b*, 209–214.
[52] B. R. Srinivasan, B. K. Vernekar, K. Nagarajan, *Indian J. Chem.* **2001**, *40 A*, 563–567.
[53] B. R. Srinivasan, A. R. Naik, C. Näther, W. Bensch, *Z. Anorg. Allg. Chem.* **2007**, *633*, 582–588.
[54] J. Ellermeier, C. Näther, W. Bensch, *Acta Crystallogr.* **1999**, *C55*, 501–503.
[55] B. R. Srinivasan, S. N. Dhuri, A. R. Naik, C. Näther, W. Bensch, *Z. Anorg. Allg. Chem.* **2013**, *639*, 512–516.

Submitted: March 12, 2021
Accepted: May 4, 2021